



## Research Article

<https://doi.org/10.1631/jzus.A2500232>



# Experience-guided optimization of jacket foundations for offshore wind turbines in varying water depths based on finite element analysis and the genetic algorithm

Jiajia HUANG<sup>1,2</sup>, Tao JIN<sup>1</sup>, Jianwu HUANG<sup>1</sup>, Shasha SONG<sup>3,4</sup>, Wei DAI<sup>1</sup>, Chaoqun ZUO<sup>1</sup>, Lizhong WANG<sup>2</sup>, Lilin WANG<sup>5✉</sup>, Zhen GUO<sup>2</sup>

<sup>1</sup>China Energy Engineering Group Zhejiang Electric Power Design Institute Co., Ltd., Hangzhou 310012, China

<sup>2</sup>College of Civil Engineering and Architecture, Zhejiang University, Hangzhou 310058, China

<sup>3</sup>College of Civil Engineering, Tongji University, Shanghai 200092, China

<sup>4</sup>School of Civil Engineering, Shaoxing University, Shaoxing 312000, China

<sup>5</sup>Ocean College, Zhejiang University, Zhoushan 316021, China

**Abstract:** Structural optimization plays a crucial role in reducing the cost of offshore wind power, particularly in deep-water regions where the weight of jacket foundations increases substantially. However, there is ongoing debate regarding the water-depth range that is suitable for jacket foundations, and the threshold where floating foundations become more viable. Existing studies have not quantitatively analyzed how water depth affects jacket foundation mass, and have often struggled to handle the high dimensionality and stringent constraints inherent in jacket foundation optimization problems. In this study, we propose an optimization framework that couples parametric finite element analysis with a genetic algorithm to minimize the mass of jacket foundations based on three actual engineering projects at varying water depths. A novel population initialization strategy incorporating engineering experience-based solutions is introduced to improve convergence efficiency and solution quality. Comparative analysis against preliminary designs and existing offshore wind projects demonstrates the model's ability to achieve cost-effective solutions, specifically reducing required jacket masses by 18.66%, 20.98%, and 17.22% at depths of 30.06, 60.23, and 89.81 m, respectively. The results reveal a 122.94% increase in jacket mass—from 1431.28 to 3190.90 t—as water depth increases from 30.06 to 89.81 m. The jacket foundation demonstrates superior cost effectiveness in shallow to moderate water depths, as the unit weight per megawatt (MW) of floating foundations is 97.51% and 35.74% higher at water depths of 60.23 and 89.81 m, respectively. Accordingly, the applicable water-depth threshold between the jacket and floating foundations is estimated to be approximately 100 m. The proposed optimization model offers a novel methodology and practical insights for the optimal design of offshore wind turbine support structures in varying marine environments.

**Key words:** Structural optimization; Jacket foundation; Genetic algorithm; Offshore wind power; Population initialization; Parametric modeling

## 1 Introduction

Offshore wind power (OWP), with its stable wind resources, low environmental impact, and proximity to demand centers (Li et al., 2022), has become a strategic priority in coastal regions. Over the next decade, an additional 411.5 GW of new capacity is projected,

with annual growth expected to average 25% in the first five years (Williams and Zhao, 2024). As critical components of OWP systems, offshore wind turbine (OWT) foundations are essential for ensuring structural safety and managing construction costs, typically accounting for approximately 25% of the total project expenditure (Gavin et al., 2011; Oh et al., 2018). OWT foundations are generally classified into two main categories based on the way they are anchored to the seabed: fixed foundations and floating foundations. Fixed foundations are typically employed in shallow to medium water depths, including gravity-based foundations (Esteban et al., 2015, 2019), monopile foundations

✉ Lilin WANG, [lilin.wang@zju.edu.cn](mailto:lilin.wang@zju.edu.cn)

Jiajia HUANG, <https://orcid.org/0000-0002-4816-4560>

Received June 5, 2025; Revision accepted Sept. 4, 2025;  
Crosschecked Dec. 31, 2025; Online first Jan. 22, 2026

© Zhejiang University Press 2026

(Achmus et al., 2009; Jindal et al., 2024), suction bucket foundations (Grecu et al., 2021; Cheng et al., 2024), and jacket foundations (Shi et al., 2013; Jalbi and Bhattacharya, 2020; Du et al., 2023). In contrast, floating foundations are designed for deeper waters (Liu et al., 2016; Hong et al., 2024). As OWP development advances into deeper and more remote waters, the choice between jacket foundations and floating foundations has become a critical and challenging decision. According to the consultancy company Xodus Group Limited (Pirainen et al., 2020), jacket foundations were more cost-effective than floating foundations at depths up to 90 m, with this advantage likely to remain at depths up to 65 m by 2030. This view is now widely accepted, with jacket foundations regarded as the preferred solution in water depths of up to 80 m.

Current design practices for jacket foundations often involve considerable structural redundancy, indicating significant potential for optimization. As wind farm development progresses into deeper waters, the weight of the jacket foundation increases substantially, leading to a marked decline in cost-efficiency. In this context, structural optimization becomes increasingly critical. Effective optimization strategies not only help reduce construction and material costs but also expand the applicable depth range of jacket foundations. Structural optimization is a design methodology that seeks the optimal configuration under predefined objectives and constraints, and it can be broadly categorized into two types. The first is conventional optimization, which consists of three subtypes: size optimization (Chew et al., 2016), shape optimization (Feng et al., 2000), and topology optimization (Tian et al., 2022; Rizk-Allah et al., 2024; Zhou et al., 2025). Size optimization treats the dimensional parameters as design variables. It is typically employed during the detailed design stage and can enhance the manufacturability of the final product. Shape optimization focuses on modifying the geometry of a structure's external boundaries, often to improve its performance under specific load or deformation constraints. It is particularly effective in reducing stress concentrations and improving fatigue life. In topology optimization, conceptual layouts that differ from a structure's initial form are generated, which fundamentally change the force transfer paths in the structure to improve its effectiveness (Wang et al., 2023). As an example of innovation in these fields, Yu et al. (2023) proposed a novel reliability-based design optimization

method that combined topology, shape, and size optimization to design an improved jacket support structure for OWTs.

The second category is heuristic optimization algorithms, which have demonstrated high efficacy in addressing large-scale and complex structural optimization problems. In the context of marine engineering structures, commonly used heuristic algorithms include ant colony optimization (ACO) (Luh and Lin, 2008), particle swarm optimization (PSO) (Li et al., 2024; Benítez-Suárez et al., 2025), and genetic algorithm (GA) (Gentils et al., 2017; Syalsabila et al., 2022). ACO is inspired by the foraging behavior of ants and is well-suited for solving combinatorial optimization, path planning, and scheduling problems. GA shows significant advantages in solving multi-objective optimization problems due to its robustness and flexibility, making it particularly suitable for scenarios involving many design variables (Saka et al., 2025). For instance, Gentils et al. (2017) proposed a GA-based optimization framework for OWT foundation structures, integrating parametric finite element (FE) modeling to simultaneously optimize the outer diameter and wall thickness of structural components. Similarly, Alhamaydeh et al. (2017) applied GA to optimize truss structures, achieving optimal configurations of end-node positions and cross-sectional areas under combined conditions of wind, wave, and seismic loading. PSO simulates the foraging behavior of bird flocks to achieve cooperative evolution of particles in the search space. It is well-suited for continuous and nonlinear optimization problems, offering strong adaptability and broad applicability. Benítez-Suárez et al. (2025) presented a PSO-based framework to optimize jacket structures for OWTs in order to improve both performance and cost. Their research integrated precomputed candidate solution clusters with multi-objective constraint mechanisms, making the methodology particularly suitable for complex structural spaces.

Single heuristic algorithms often fall short when applied to complex structural systems due to premature convergence, local optima, or limited search ability. To address these challenges, researchers have developed more robust and efficient hybrid optimization methods, such as the GA-PSO hybrid strategy (Duan et al., 2022) and the marine predator algorithm (MPA)-PSO hybrid algorithm (Shemshaki et al., 2025); these approaches are especially effective for high-dimensional

and constrained problems. Despite the proven potential of heuristic optimization algorithms for structural design of marine engineering systems, challenges remain in applying them to high-dimensional and highly constrained jacket foundation optimization problems. These challenges particularly manifest in terms of poor population initialization quality and limited convergence efficiency. Moreover, existing studies demonstrate insufficient rigor in adhering to engineering design procedures and provide limited quantitative assessments on the influence of water depth on jacket foundation mass. Meanwhile, the threshold water depth for the jacket in floating foundations remains a subject of debate.

In this study, we propose an experience-guided optimization framework for jacket foundations of OWTs based on three practical engineering cases located at three different water depths (30.06, 60.23, and 89.81 m). The approach integrates parametric structural modeling using a structural analysis computer system (SACS) with a GA-based optimization scheme, aiming to improve the design efficiency and structural performance. To overcome the challenges associated with high-dimensional variables and stringent design constraints, a problem-specific initialization strategy is employed to enhance the quality and convergence of the optimization. Furthermore, a comparative investigation of the optimized designs corresponding to shallow-, intermediate-, and deep-water scenarios is conducted, elucidating the impact of water depth on jacket configuration, and offering practical insights for foundation design in complex offshore environments.

## 2 Overview of the engineering projects

This study is based on three representative engineering projects located along China's coastal region, which offer rich datasets and practical relevance for the optimization of jacket foundations. This robust engineering context provides a sound basis for the development of jacket foundation optimization methods.

The design of offshore jacket foundations is closely related to local marine hydrographic conditions, which determine the environmental loading parameters that are essential for structural analysis. These conditions encompass design water levels and wind, wave, and current characteristics, which together define the boundary

conditions for evaluating the ultimate strength, fatigue life, and overall stability of the foundation. For clarity and conciseness, the detailed descriptions, data sources, and tabulated values of these marine environmental factors are presented in Section S1 of the electronic supplementary materials (ESM).

For the purpose of comparative analysis, the geological conditions adopted for all projects are based on the data from Project A. According to the borehole survey results of Project A, from top to bottom, the primary soil layers include mud, silt, silty clay, fine sand, and fine to medium sand, with considerable variations in layer thickness due to depositional heterogeneity. A detailed description of the stratigraphic distribution and geotechnical properties is presented in Table S6 of the ESM.

## 3 Parametric finite element model for jacket foundation

A FE model was developed to simulate the structural behavior of the offshore jacket foundation under realistic marine environmental and geological conditions. The model incorporates the overall structural configuration, the environmental and operational loads, representative design load cases, and nonlinear pile–soil interaction, thereby establishing a framework for evaluating strength, serviceability, and fatigue performance. To maintain clarity in the main text, a more detailed description of the FE model of the jacket foundation is presented in Section S2 of the ESM.

To support the structural optimization process driven by a GA, a fully parametric FE modeling framework for jacket foundations is established using Python within the SACS software environment. The modeling process—including geometry generation, material assignment, load application, boundary condition definition, etc.—is entirely automated through customized Python routines. This enables dynamic modification of structural configurations and high-throughput evaluation of multiple design scenarios within an iterative optimization loop. The model comprehensively addresses both ultimate limit state (ULS) and fatigue limit state (FLS) conditions, ensuring structural integrity under extreme environmental loads and long-term cyclic actions. The Python-based post-processing system automatically extracts key structural responses, including

unity check (UC) values, model frequencies, and fatigue life, so as to support comprehensive design verification. This end-to-end automation process—going from model generation to post-analysis verification—greatly enhances the computational efficiency and scalability of our structural optimization method. This framework enables a rapid and reliable assessment of a broad range of jacket foundation designs under realistic environmental loadings, aiding experience-guided optimization workflows.

## 4 Optimization model integrating the genetic algorithm and parametric finite element modeling

### 4.1 Genetic algorithm overview

In this study, a GA (Goldberg, 1989) is employed as the core optimization strategy in the optimization design of an OWT jacket foundation. As a population-based stochastic optimization technique, GA is inspired by the mechanisms of natural selection and genetic inheritance observed in biological evolution. Through iterative applications of selection, crossover, and mutation operators, the algorithm progressively refines candidate solutions towards a global optimum. The overall computational framework of the GA implemented in this study is depicted in Fig. 1. Due to its strong global search capability, GA demonstrates a distinct advantage in handling complex optimization landscapes

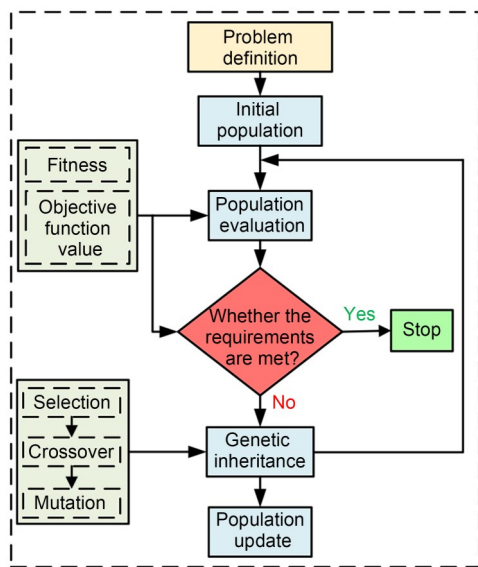


Fig. 1 Flowchart of the genetic algorithm

characterized by nonlinearity, multimodality, and multiple design constraints. It has been widely applied (Gentils et al., 2017; Syalsabila et al., 2022; Saka et al., 2025) in structural optimization problems where traditional gradient-based approaches often struggle, such as the structural optimization of OWT jacket foundations.

### 4.2 Formulation and configuration of the experience-guided optimization model

By integrating the parametric SACS-based analysis model of OWT jacket foundations with a GA, an experience-guided optimization framework is established to enable automated design, analysis, and iterative optimization.

#### 4.2.1 Objective function and design variables

The objective of the proposed optimization model is to minimize the total mass of the jacket foundation  $M_{jcp1}$  which comprises the mass of the upper jacket structure  $M_{jack}$  and the mass of the pile foundation  $M_{pile}$ . The objective function  $F_{obje}$  can therefore be expressed as follows:

$$F_{obje} = \min(M_{jcp1}) = \min(M_{jack} + M_{pile}). \quad (1)$$

To achieve this goal, a set of structural design variables is defined and optimized within the GA framework. The optimization design variables can be categorized into six groups: (1) top and bottom leg spacings; (2) main leg diameters; (3) main leg wall thicknesses; (4) diameters of diagonal bracing members; (5) wall thicknesses of diagonal bracing members; (6) pile-related parameters, including embedded depth, diameter, and wall thickness. These parameters are treated as discrete variables depending on the design requirements and are bounded by structural safety criteria, manufacturing limitations, and practical engineering constraints.

There are three engineering projects with different water depths, which are investigated for optimization. The third project case (Project C, with a water depth of 89.81 m and 27 optimization variables) is selected as a representative example to detail the optimization design variables, as shown in Fig. 2. Here,  $x_j$  ( $j = 1, 2, \dots, 27$ ) is the  $j$ th optimization design variable;  $L_{top}(x_1)$  is the top leg spacing;  $L_{bott}(x_2, x_1)$  is the bottom leg spacing;  $L_{empl}(x_{25})$  is the embedded depth of pipe;  $D_{pile}(x_{26})$  is the pile diameter;  $t_{pile}(x_{27})$  is the maximum wall thickness of the pipe.  $D_{leg0}(x_3)$  and  $t_{leg0}(x_9)$  are the

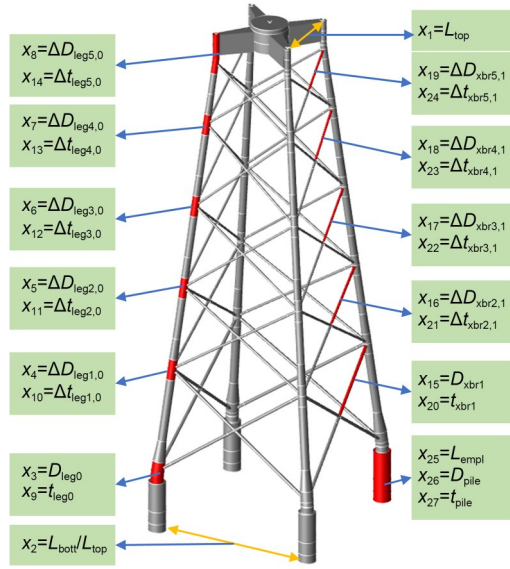


**Fig. 2 Schematic diagram of the 27 optimization design variables for the jacket foundation in Project C**

diameter and wall thickness of the bottom main leg, respectively;  $\Delta D_{legi,0}$  ( $i=1, 2, \dots, 5$ ) is the difference between the main leg diameter at the  $i$ th layer  $D_{legi}$  and that of the bottom layer (i.e.,  $\Delta D_{legi,0}=D_{legi}-D_{leg0}$ , corresponding to  $x_4-x_8$ );  $\Delta t_{legi,0}$  is the difference between the main leg wall thickness at the  $i$ th layer  $t_{legi}$  and that of the bottom layer (i.e.,  $\Delta t_{legi,0}=t_{legi}-t_{leg0}$ , corresponding to  $x_{10}-x_{14}$ ).  $D_{xbr1}$  ( $x_{15}$ ) and  $t_{xbr1}$  ( $x_{20}$ ) are the diameter and wall thickness of the diagonal bracing members, respectively;  $\Delta D_{xbr,i}$  ( $i=2, 3, 4, 5$ ) is the diameter difference between the diagonal bracing member at the  $i$ th layer  $D_{xbr,i}$  and that of the bottom layer (i.e.,  $\Delta D_{xbr,i}=D_{xbr,i}-D_{xbr1}$ , corresponding to  $x_{16}-x_{19}$ );  $\Delta t_{xbr,i}$  is the wall thickness difference between the diagonal bracing member at the  $i$ th layer  $t_{xbr,i}$  and that of the bottom layer (i.e.,  $\Delta t_{xbr,i}=t_{xbr,i}-t_{xbr1}$ , corresponding to  $x_{21}-x_{24}$ ). A typical jacket layer, with its geometric configuration and associated optimization

design variables, is illustrated in Fig. S6 of the ESM. Notably, the number of layers and layer heights are not set as optimization variables. The jacket foundation in Project C consists of five layers, and according to engineering design experience, the relative height proportions of each layer compared to the total structural height are set as 0.25, 0.20, 0.20, 0.20, and 0.15, respectively, from bottom to top. Three layers with height ratios of 0.40, 0.30, and 0.30 are used for Project A, and four layers with height ratios of 0.30, 0.30, 0.20, and 0.20 are used for Project B.

Fig. 3 presents a top view of the jacket and the geometric configuration of the pile foundation with its associated optimization design variables. The pile foundation involves three key variables: the embedded depth  $L_{empl}$ , the pile diameter  $D_{pile}$ , and the maximum wall thickness  $t_{pile}$ . The pile is composed of multiple segments with varying wall thicknesses. The detailed lengths and thicknesses of the segments are illustrated in Fig. 3b. All design variables are treated as integers that vary in discrete steps, with the lower and upper bounds given as integer multiples of the step size. For the three projects, the detailed step sizes, along with the corresponding lower and upper integer bounds for each variable, are provided in Table S7 of the ESM. Accordingly, the feasible search space only consists of discrete integer points, and all candidate solutions are generated within these bounds.

#### 4.2.2 Design constraints

The structural configuration, ultimate bearing capacity, frequency, and fatigue life of the jacket foundation must comply with relevant design codes. Based on these specifications, the constraint conditions for the optimization model of the jacket foundation are defined as follows:

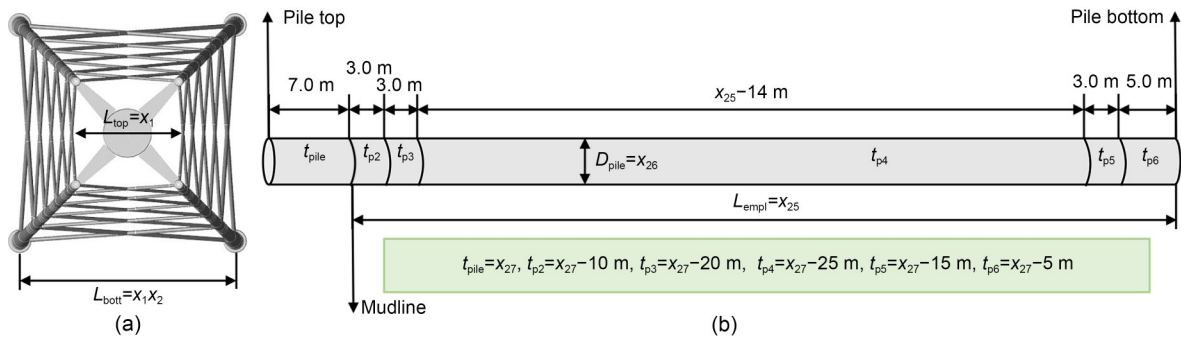


**Fig. 3 Structural layout and associated optimization design variables of the jacket foundation: (a) top view of the jacket; (b) geometric configuration of the pile foundation**

(1) Strength and stability constraints

These constraints ensure that all jacket members, joints, and pile shafts have sufficient strength. The UC value is defined as the ratio between the applied load effect and the corresponding design resistance specified in the governing codes (API, 2019a, 2019b; DNV, 2021). It is verified in this study using the SACS code-check module. The UC values for the jacket members, joints, and pile shaft stress must be smaller than 1.0 under extreme loading conditions:

$$U_{mem}, U_{jold}, U_{josr}, U_{pile} < 1.0, \quad (2)$$

where  $U_{mem}$  is the UC value of the jacket member;  $U_{jold}$  and  $U_{josr}$  are the load UC value and strength UC value of the joint, respectively;  $U_{pile}$  is the shaft stress UC value of the pile. Further details on the definitions of these UC values are presented in Section S3 of the ESM.

(2) Compressive and uplift bearing capacities of the pile foundation

According to American Petroleum Institute (API) codes, the safety factor for compressive or uplift bearing capacity of the pile foundation must be greater than 1.25 under extreme loading conditions:

$$S_{comp}, S_{upft} > 1.25, \quad (3)$$

where  $S_{comp}$  and  $S_{upft}$  are the safety factors for compressive and uplift bearing capacities of the pile, respectively, which are defined as the ratios of the pile capacities to the applied pile loads.

(3) Fatigue life constraint

The fatigue life of critical members  $F_{crit}$  must be greater than the target design life, which is typically 25 a for OWT foundations:

$$F_{crit} > 25 \text{ a}. \quad (4)$$

(4) Frequency constraint

To avoid resonance, the first natural frequency  $f_{1st}$  of the structure must fall within the allowable frequency range (0.195–0.220 Hz) provided by the wind turbine manufacturer. In this study, the range is:

$$0.195 \text{ Hz} < f_{1st} < 0.220 \text{ Hz}. \quad (5)$$

(5) Geometric constraint

The grout thickness  $t_{grout}$  in the grouted connection between the upper jacket structure and the pile

foundation (Fig. 4) is required to exceed 250 mm, so as to ensure adequate load transfer and structural integrity:

$$t_{grout} \geq 250 \text{ mm},$$

$$\text{i.e., } \begin{cases} x_{18} - 2x_{19} - x_3 \geq 2 \times 250 \text{ mm, for Project A,} \\ x_{22} - 2x_{23} - x_3 \geq 2 \times 250 \text{ mm, for Project B,} \\ x_{26} - 2x_{27} - x_3 \geq 2 \times 250 \text{ mm, for Project C.} \end{cases} \quad (6)$$

Also, the pile wall thickness must exceed a minimum threshold relative to the pile diameter to prevent local buckling. Specifically, a geometric constraint is applied such that the pile wall thickness satisfies the condition:

$$t_{p, \min} \geq \frac{D_{pile}}{120},$$

$$\text{i.e., } \begin{cases} x_{19} - 25 \text{ mm} \geq \frac{x_{18}}{120}, \text{ for Project A,} \\ x_{23} - 25 \text{ mm} \geq \frac{x_{22}}{120}, \text{ for Project B,} \\ x_{27} - 25 \text{ mm} \geq \frac{x_{26}}{120}, \text{ for Project C,} \end{cases} \quad (7)$$

where  $t_{p, \min}$  is the minimum wall thickness of the pile, taken as  $x_{19} - 25$  mm,  $x_{23} - 25$  mm, and  $x_{27} - 25$  mm for Projects A, B, and C, respectively.

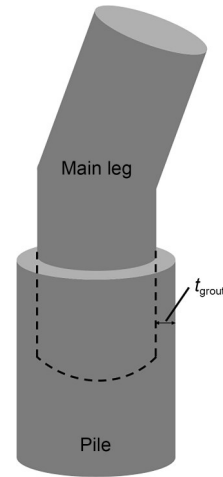


Fig. 4 Schematic diagram of the grouted connection between the upper jacket structure and the pile

(6) Design variable constraint

To ensure a feasible and realistic design, each design variable is constrained to vary within a range defined by the upper bound  $x_j^U$  and lower bound  $x_j^L$ :

$$x_j^L \leq x_j \leq x_j^U. \quad (8)$$

The optimization model considers constraints from design codes, structural detailing requirements, and auxiliary conditions. These are applied in two steps. First, constraints not related to finite element analysis (FEA) are checked within the population, and any infeasible solutions are assigned a large penalty value (e.g., 9999) to exclude them from further evaluation. Second, the remaining solutions undergo FE analysis, and their results are verified against the code-based requirements in Eqs. (2)–(5). Solutions failing these checks receive another large penalty value. This penalty-based approach ensures that only solutions that meet all stringent constraints are retained during the optimization.

#### 4.2.3 Population initialization based on engineering experience and constraints

To ensure diversity and constraint feasibility during the early stages of the GA, a hybrid population initialization strategy is developed. The approach utilizes integer design variables (all design variables are defined as integer variables with discrete step sizes, reflecting standardized increments in engineering design and manufacturing practice) and nonlinear constraints; it also integrates engineering experience, controlled perturbations, and Latin hypercube sampling (LHS). The overall workflow is illustrated in Fig. 5. The population is divided into three components: expert solutions (feasible candidate solutions obtained in advance based on engineering design experience), perturbed solutions generated around expert solutions, and LHS-based solutions that are generated randomly. The number of individuals in each component is calculated to match the total population size. Expert solutions are first added to the population directly. These solutions provide a high-quality baseline for exploration of the search space. Around each expert solution, a number of perturbed individuals are created by applying random deviations scaled by variable-wise perturbation factors. These perturbed individuals are bounded, rounded, and retained only if they satisfy the non-FEA-related constraints. To improve diversity, a portion of the population is generated via LHS. Random individuals are uniformly sampled within the feasible integer bounds and accepted only if they meet all non-FEA-related constraints. This hybrid strategy, integrating engineering experience-based solutions, can enhance convergence and improve solution quality in early iterations, making it particularly advantageous for complex engineering optimization problems

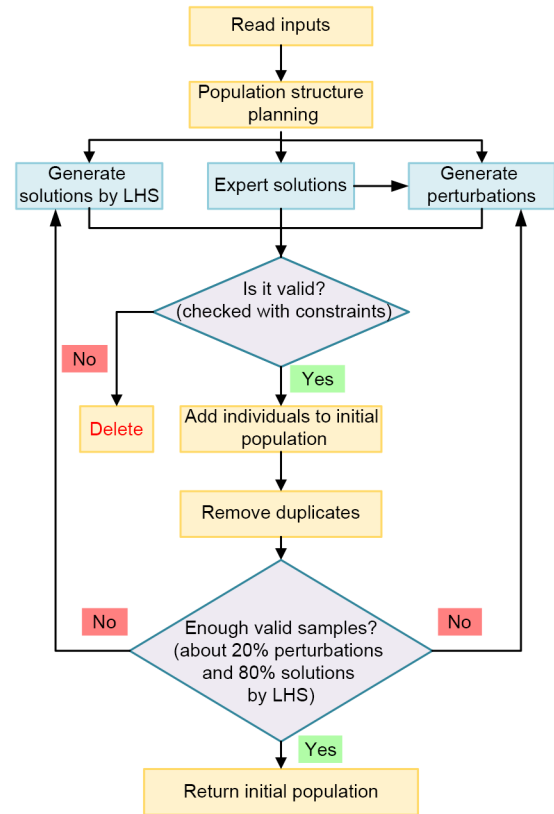


Fig. 5 Overall workflow of the population initialization process

characterized by high-dimensional design variables and stringent constraints.

#### 4.3 Optimization workflow integrating genetic algorithm and parametric finite element modeling

Fig. 6 depicts a flowchart of the optimization model for the jacket foundations of OWTs, which combines parametric FE and GA modules. In the FE analysis module, a Python-based parametric modeling program is developed for jacket foundations using the SACS platform, enabling automated generation of input files for analysis. The modeling process is encapsulated into reusable function modules. A Python interface is then implemented to invoke the SACS solver for structural analysis. Finally, a result post-processing submodule is developed to identify errors, extract key output parameters, and perform quality checks. In the GA module, the optimization objective, design variables, and constraint conditions are clearly defined. An engineering experience-guided strategy is adopted for population initialization to enhance the feasibility and diversity of solutions. The SACS-based FE analysis module is then

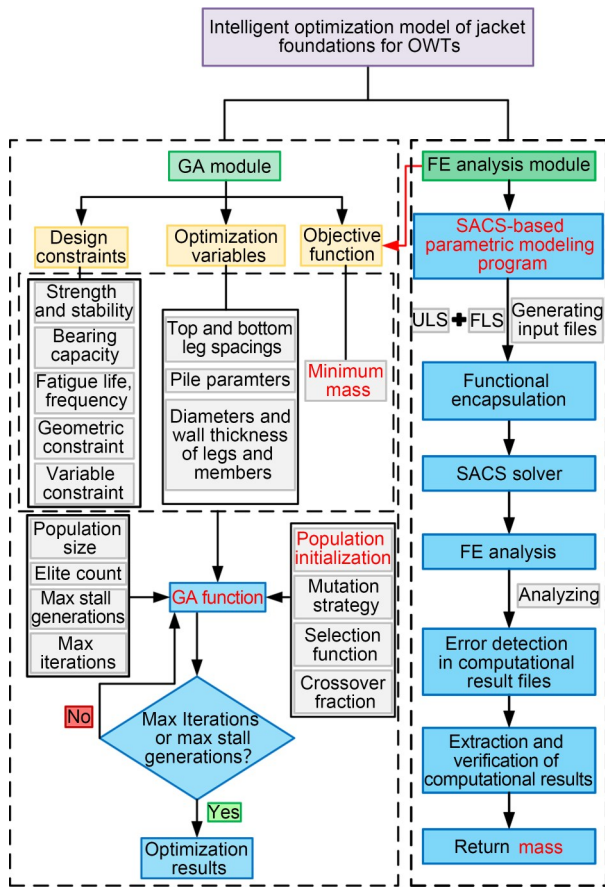


Fig. 6 Flowchart of the experience-guided optimization model integrating GA and parametric FE modeling for jacket foundations

embedded into the GA framework to enable iterative optimization of the jacket foundation.

#### 4.4 Parameter settings for the genetic algorithm

Based on the oceanographic, geotechnical, and wind turbine load parameters from the three real offshore engineering projects (Projects A, B, and C) with different water depths, optimization design of the jacket foundations for OWTs was carried out for each project. The optimization process was configured with 100 generations and a population size of 50 individuals per generation. The convergence criteria were set as either reaching a maximum of 15 stagnant generations or completing all iterations. Each generation retained five elite individuals for the next generation. The crossover rate was 0.8. The mutation strategy employed was adaptive feasible mutation, which dynamically adjusts the mutation steps based on the feasibility of individuals, thereby ensuring that the offspring remain within constraints

and promoting efficient convergence toward the optimal solution. The employed selection method was tournament selection, which extracts the best individual from a randomly chosen subset of the population, thus enhancing selection pressure and accelerating convergence toward high-quality solutions. The initial population was generated in accordance with the proposed initialization strategy. The optimization model used the total mass of the jacket foundation (i.e., the sum of the jacket mass and the pile foundation mass) as the fitness evaluation criterion.

## 5 Results and discussion

For the optimization runs (100 generations with a population size of 50), the total computational time was about 125 h on a workstation with 32 GB RAM and a single-core CPU. A complete FE analysis of a single design required approximately 3 min (about 70 s for ULS and 110 s for FLS). Due to pre-screening of infeasible candidates and additional filtering after ULS evaluation, only about 25% of individuals underwent both ULS and FLS checks; this reduced the computational burden.

### 5.1 Analysis of jacket foundation mass optimization

Minimizing the jacket foundation mass is a key objective in the design of cost-effective support systems for OWTs. The evolution of the jacket foundation masses for Projects A, B, and C is presented in Fig. 7. By incorporating a small number of feasible solutions based on engineering experience, Projects A, B, and C began the optimization process with initial masses of 1917.96, 2971.08, and 4256.38 t, respectively. The hybrid initialization strategy ensured that the optimization process could be initialized from a feasible starting point in terms of the complex conditions of real engineering problems. The overall trend indicates that the most significant mass reduction occurs during the initial phase of the optimization process and is followed by a gradual convergence toward an optimal design  $M_{opt}$ . In the first 20 generations, the structural mass was reduced by 22.24%, 19.67%, and 15.36% for Projects A, B, and C, respectively, which accounted for 87.65%, 62.54%, and 61.37% of their total mass reductions achieved at convergence. Project A exhibited a significantly faster convergence rate compared to Projects B and C, due

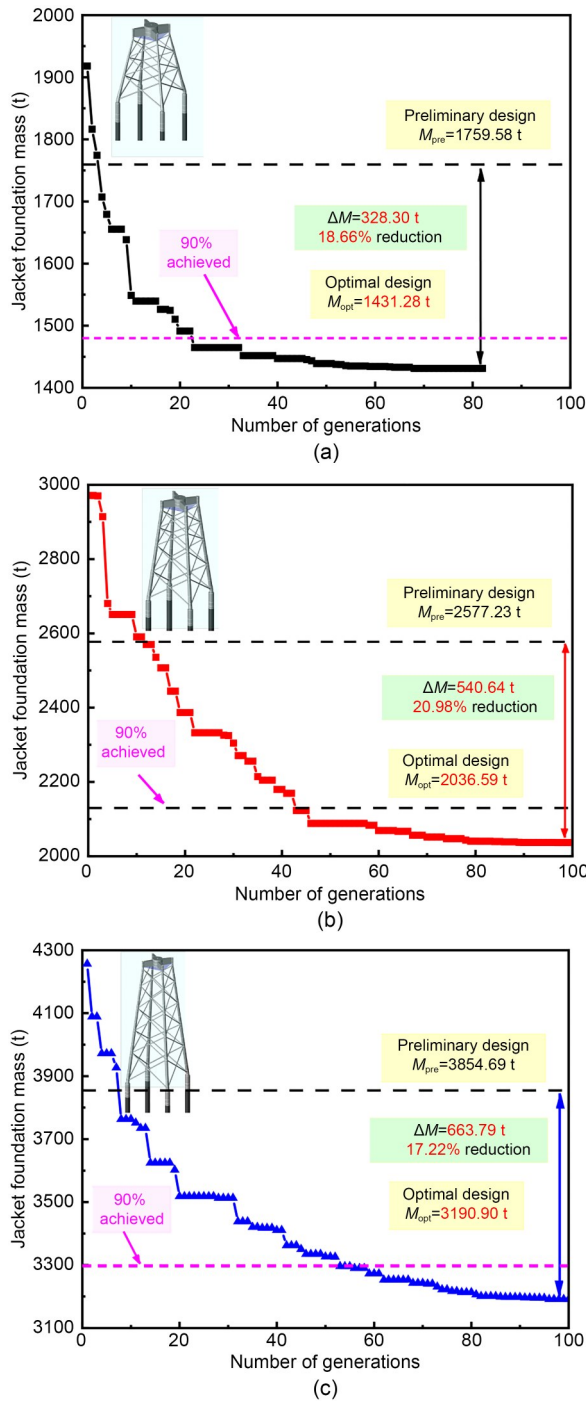


Fig. 7 Optimization process of the jacket foundation mass via GA iterations: (a) Project A; (b) Project B; (c) Project C

to its smaller number of design variables (19 compared to 23 and 27, respectively). To achieve 90% of the total mass reduction, Projects A, B, and C required 23, 43, and 53 generations, respectively. At the three water depths of 30.06, 60.23, and 89.81 m, the optimized total jacket foundation masses  $M_{opt}$  were 1431.28, 2036.59,

and 3190.90 t, respectively. These represent mass reductions  $\Delta M$  of 328.30 (18.66%), 540.64 (20.98%), and 663.79 t (17.22%) compared to the preliminary designs  $M_{pre}$ , which had respective masses of 1759.58, 2577.23, and 3854.69 t. These results demonstrate the effectiveness of the proposed optimization framework across varying water depths.

Fig. 8 presents a comparison between the optimized jacket foundation design and those of other offshore wind power projects already in operation with similar water depths. Compared to Project HZGK (water depth: 31.90 m) and Project PTA (water depth: 30.58 m), the optimized design achieved mass reductions of 28.74% and 15.18%, corresponding to steel savings of 577.12 and 256.13 t, respectively. These results clearly demonstrate the effectiveness of the proposed optimization model in reducing structural mass, as validated against real offshore wind power projects under comparable site conditions. Furthermore, this comparison emphasizes that thoughtful application of heuristic optimization techniques—particularly those integrating engineering experience-based solutions and constraint handling—can yield substantial improvements over traditional preliminary design practices.

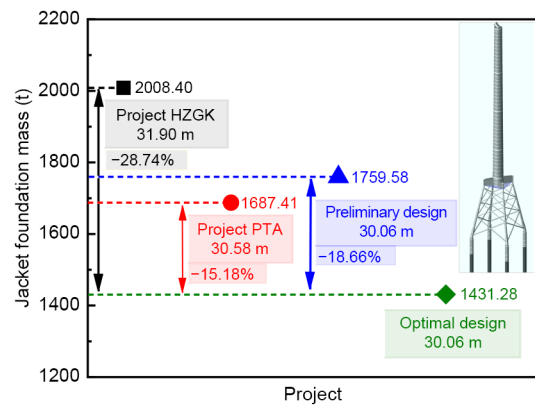
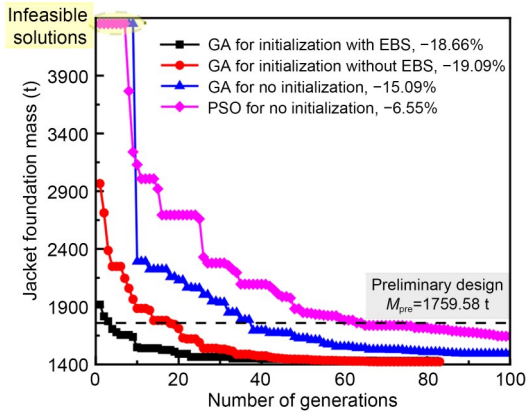


Fig. 8 Comparison between the optimal jacket foundation mass and those of other offshore wind projects

### 5.2 Influence of initialization strategy and algorithm choice

Fig. 9 presents a comparison of optimization performance with different initialization strategies: no initialization, initialization without the incorporation of experience-based solution (EBS), and initialization incorporating EBS. From the overall convergence trend, it is clear that the no-initialization strategy generated a large proportion of infeasible solutions during the early



**Fig. 9 Comparison between optimization performance among GA with different initialization strategies and PSO without initialization**

iterations (with no feasible solutions produced in the first nine generations), resulting in low exploration efficiency and slow improvement in mass reduction. In contrast, the initialization strategy incorporating EBS substantially reduced the proportion of infeasible solutions in the early stage and provided a feasible optimization starting point of 1917.96 t, leading to a much faster initial convergence rate. The convergence rate achieved with the second initialization strategy (initialization without EBS) was intermediate between the other two approaches. This demonstrates that the initialization strategy incorporating EBS is highly beneficial for complex engineering optimization tasks, as it ensures early feasibility, provides a high-quality starting point, and maintains exploration through LHS, thereby accelerating convergence and improving solution quality. Fig. 9 also showcases a comparison of optimization performance between GA and PSO. GA demonstrates superior performance compared to PSO for the jacket foundation, achieving a structural mass reduction of 15.09%, compared to only 6.55% for PSO. PSO is more likely to suffer from premature convergence due to its weaker global search capability, whereas GA demonstrates stronger global exploration ability, along with better handling of discrete design variables and complex nonlinear constraints; this makes it more suitable for large-scale structural optimization tasks, such as optimization of jacket foundations.

### 5.3 Analysis of design constraints in the optimization

An in-depth examination of the design constraints is conducted to identify the most critical factors influencing the structural design. A total of nine design

constraints were incorporated into the GA framework to ensure structural safety, serviceability, and compliance with offshore engineering standards. These include the jacket member UC value  $U_{mem}$ , the load and strength UC values of the joint  $U_{jold}$  and  $U_{jost}$ , the shaft stress UC values of the pile under compressive and uplift loading  $U_{pls}$  and  $U_{plu}$ , the safety factors for compressive and uplift bearing capacities of the pile  $S_{comp}$  and  $S_{uplt}$ , the fatigue life  $F_{crit}$ , and the first natural frequency  $f_{1st}$ . The evolution of the design constraints for the three projects (A, B, and C) is recorded and illustrated in Fig. 10. In all three projects, the fatigue approaches the limit value, indicating that fatigue damage is a controlling constraint under both deep- and shallow-water conditions. In Project C, and especially in Project B, the first natural frequency approaches the limit value, suggesting that frequency constraints are more critical in deep-water conditions. Regarding the pile foundation bearing capacity, uplift bearing capacity is typically the controlling constraint for pile foundation design. The uplift bearing capacity factors for Projects A and B both approach the lower limit, and Project C is also close to this limit. Member UC, joint UC, and pile shaft stress UC are generally not considered as controlling constraints, with the exception of the jacket member UC value in Project A, which approached its upper limit during the iterative optimization. In summary, the optimization process is predominantly constrained by the dynamic performance (the first natural frequency) and the fatigue durability of the jacket foundation. The analysis of the design constraints emphasizes the crucial role that these parameters play in guiding the optimization towards a feasible and efficient design.

### 5.4 Analysis of design variables in the optimization

To assess how different design parameters contribute to the optimization, the impact of selected key design variables is analyzed in this section. Figs. 11–13 present the evolution of key design variables across GA individuals for the three projects. These variables include the top and bottom leg spacings (Fig. 11), the diameters and wall thicknesses of main legs and bracing members at the top and bottom of the jacket (Fig. 12), as well as the embedded depth, diameter, and wall thickness of the pile (Fig. 13). In the course of the optimization, these variables undergo iterative adjustments to meet the imposed constraints and improve the objective function. For the top and bottom spacings of the

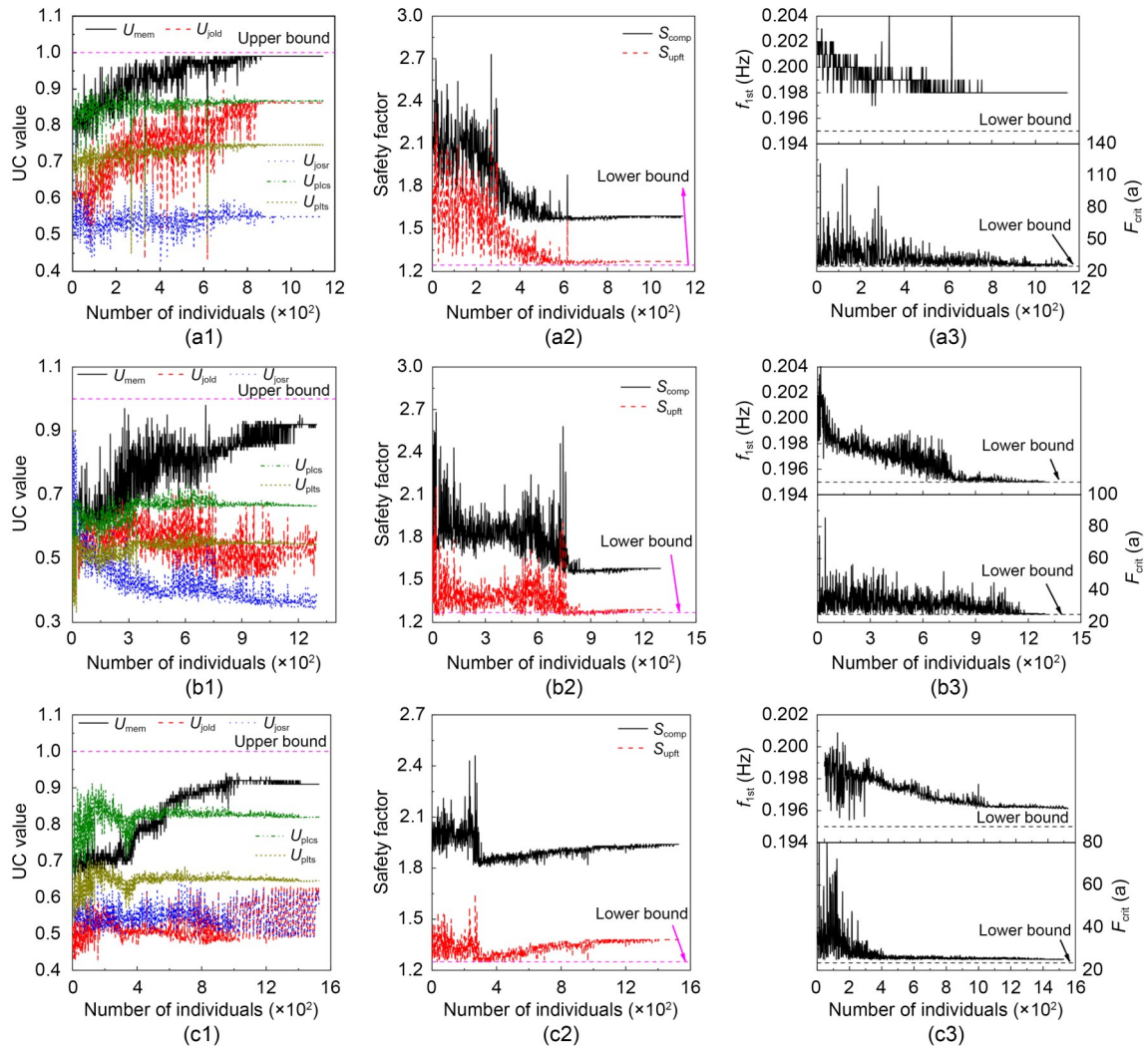


**Fig. 10** Evolution of design constraints across GA individuals for the three projects: (a1–a3) UC values, safety factors, as well as the first natural frequency and fatigue life for Project A; (b1–b3) UC values, safety factors, as well as the first natural frequency and fatigue life for Project B; (c1–c3) UC values, safety factors, as well as the first natural frequency and fatigue life for Project C

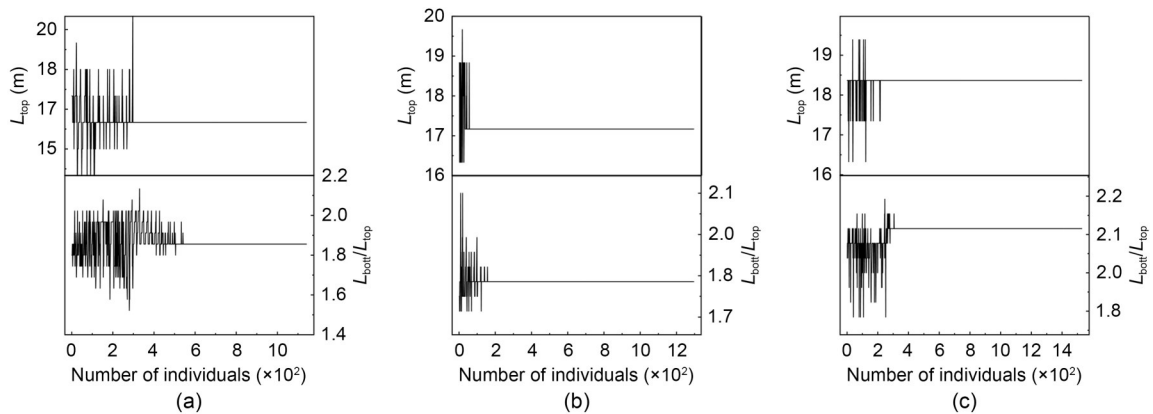


**Fig. 11** Evolution of the top leg spacing and the spacing ratio of the bottom leg to top leg across GA individuals for the three projects: (a) Project A; (b) Project B; (c) Project C

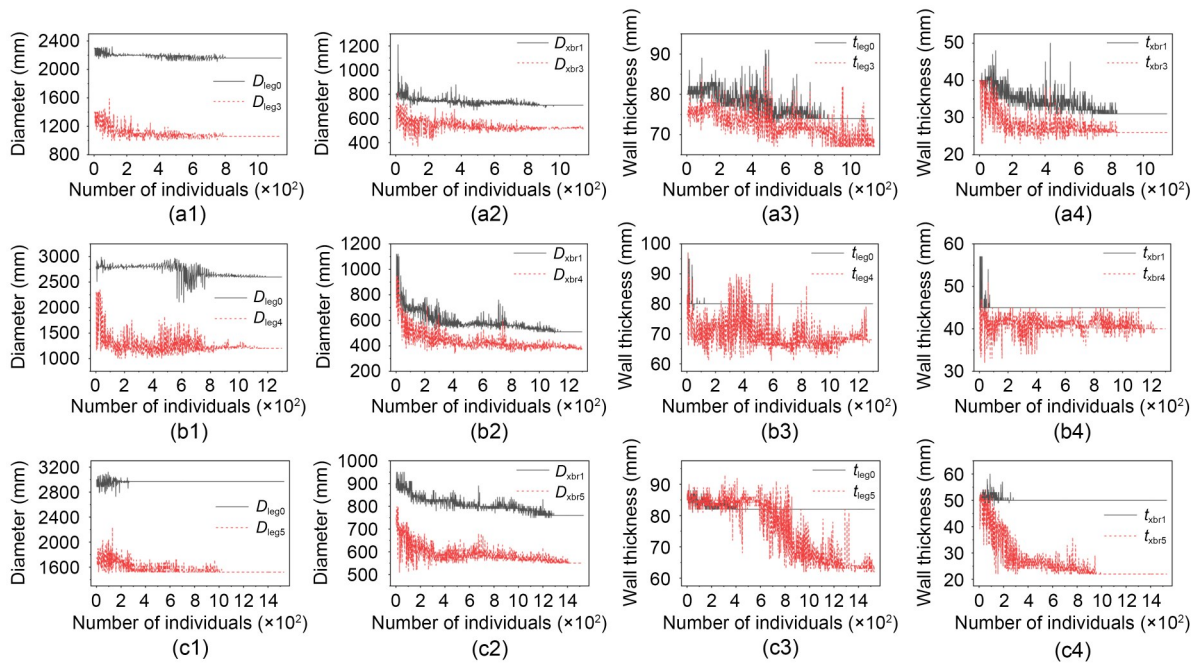


**Fig. 12 Evolution of diameters and wall thicknesses of the main legs and bracing members at the top and bottom across GA individuals for the three projects: (a1–a4) Project A; (b1–b4) Project B; (c1–c4) Project C**

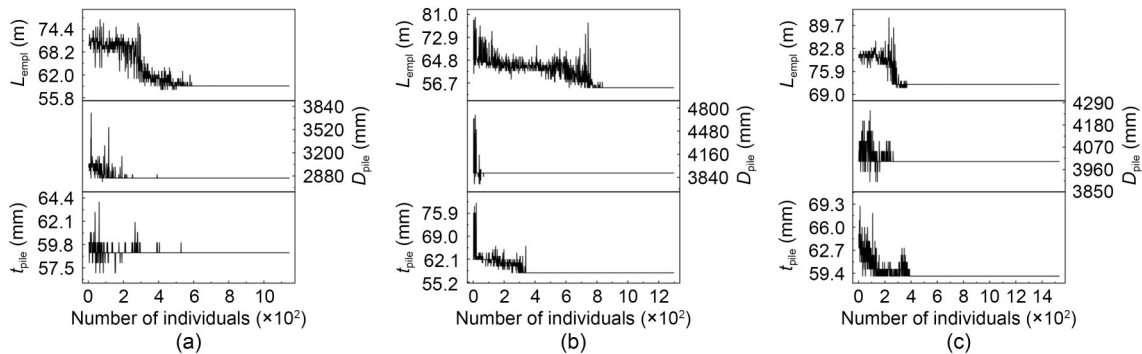


**Fig. 13 Evolution of embedded depth, diameter, and wall thickness of the pile across GA individuals for the three projects: (a) Project A; (b) Project B; (c) Project C**

jacket, they converge relatively quickly, indicating that their optimal solutions are close to the expert solution in the initial population. In contrast, the diameters and wall thicknesses of the main legs and bracing members at the top and bottom of the jacket converge more slowly, indicating that these parameters have substantial potential for further optimization. The pile foundation parameters show a moderate convergence rate.

The variational trends of design variables across individuals exhibit clear depth-dependence and convergence characteristics. First, regarding the top and bottom spacings (Fig. 11), all three datasets show a trend of transitioning from an initially scattered distribution to gradual convergence in later stages, indicating

good convergence of the GA in terms of the geometric boundary parameters. In Project A (30.06 m), the difference between the top and bottom spacings is relatively small, resulting in a gentler structural taper, whereas in Project C (89.81 m), the bottom spacing increases significantly, reflecting the higher requirements in deep-water environments for overturning resistance and base stability. As water depth increases, both the diameters and wall thicknesses of the main legs at the jacket base increase to meet the heightened demands for bending and buckling resistance. Furthermore, the pile-related diameters (Fig. 13) remain relatively consistent across all projects, whereas the wall thickness converges more slowly. Notably, in Project

C, the pile length is significantly greater than in Projects A and B, reflecting the increased demand for uplift resistance in deeper waters, which requires deeper embedding in the seabed. Overall, the water depth significantly influences the distribution characteristics of the design variables, with deeper water conditions imposing greater demands on structural strength and stability. The GA demonstrates strong adaptability, effectively balancing diversity and convergence throughout the optimization. These observed trends validate the rationality and stability of the optimization outcomes and provide essential parameter guidelines and boundary constraints for jacket structure design in varying water depths.

### 5.5 Influence of water depth on jacket foundations

Understanding how water depth influences key design parameters is essential for optimizing foundation geometry and ensuring structural safety and economic efficiency in different offshore environments. Thus, in this section, we examine the influence of water depth on jacket foundations by comparing the final optimized designs that correspond to three different water depths. All the designs were rigorously optimized using GAs and demonstrate similar fatigue lives, natural frequencies, and bearing capacity safety factors. This high degree of comparability enables us to develop insights into adaptive design strategies for projects ranging from shallow to deep water.

#### 5.5.1 Comparative analysis of jacket structure mass

Fig. 14a illustrates the variational trends of jacket mass  $M_{\text{jacket}}$ , pile foundation mass  $M_{\text{pile}}$ , total mass  $M_{\text{total}}$ , and the mass ratio of jacket to pile under different water depths. With increasing water depth, both the jacket mass and pile foundation mass show significant growth. When the water depth increases from 30.06 to 89.81 m, the jacket mass increases from 708.58 to 1999.36 t, representing a growth of 182.16%; meanwhile, the pile foundation mass increases from 722.70 to 1191.54 t, representing an increase of only 64.87%. The total weight increases from 1431.28 to 3190.90 t—an increase of 122.94%—which is significantly less than the increase in water depth (198.77%). These results indicate that water depth has a significant impact on the optimal jacket foundation mass, reflecting the enhanced structural demands imposed by deep water environments. The mass ratio of jacket to pile also increases

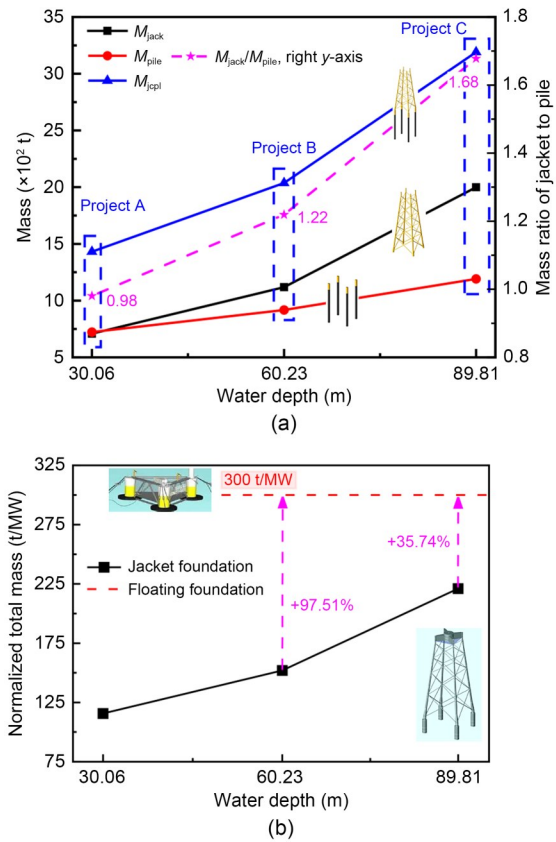


**Fig. 14 (a) Mass characteristics of jacket foundations under varying water depths; (b) comparison of normalized total mass between jacket foundations with different water depths and floating foundation**

with water depth—from 0.98 at 30.06 m to 1.68 at 89.81 m—as shown on the right y-axis in Fig. 14a, indicating that the jacket structure plays a more crucial role in deep-water conditions. Moreover, Fig. 14b presents the total mass of jacket foundations normalized per megawatt (MW) of installed capacity, plotted against water depth. This is compared with the benchmark of the most cost-effective floating foundation, which is represented by the dashed line at about 300 t/MW. Note that the reference value of 300 t/MW in this plot for floating foundations does not yet have direct support in published literature, as the lowest reported values reach approximately 350 t/MW (Li et al., 2025). However, this value is widely recognized within the industry as an advanced benchmark based on recent technical discussions and enterprise-level developments. At water depths of 60.23 and 89.81 m, the unit weight per MW of the floating foundation is 97.51% and 35.74% higher than that of the jacket foundation, respectively. Accordingly, the applicable water-depth threshold between

jacket and floating foundations is estimated to be 100 m. This comparison reveals the competitive advantage of jacket foundations over floating foundations in shallow to moderate water depths.

### 5.5.2 Model shapes and frequencies

The jacket foundation of OWT is subjected to dynamic load-induced vibrations in the structure, which generate additional stress responses within the foundation and affect the dynamic behavior of the entire system. In the design of wind turbine foundations, it is essential to consider the structural dynamics by modeling the wind turbine–tower–jacket–pile foundation–soil system as a unified dynamic mechanical model. The natural frequencies must be calculated and checked to ensure they all fall within acceptable limits, so as to prevent excessive vibrations that may impair functionality during turbine operation. Fig. 15a shows the first five model shapes of jacket foundations at different water depths. As water depth increases, the environmental loads acting on the taller jacket foundation tend to intensify, resulting in the structure vibrating with larger amplitudes. Fig. 15b presents the first 10 natural frequencies of jacket foundations at different water depths. Due to the lower bound constraint on the first natural frequency in the GA optimization, the low-order natural frequencies of the jacket foundations are not directly comparable, whereas higher-order natural frequencies can be effectively compared and analyzed. The higher-order natural frequencies are observed to decrease significantly with increasing water depth. For example, at water depths of 30.06, 60.23, and 89.81 m, the 10th natural frequencies are 2.32, 1.55, and 1.36 Hz, respectively, representing sequential decreases of 33.19% and 12.26%. Lower values of the high-order natural frequencies indicate a reduction in the structure's stiffness or increased flexibility in certain vibration modes. Overall, these effects highlight the need for careful dynamic analysis and optimization of jacket foundations in deep-water projects. These might include enhanced vibration control strategies, methods to improve stiffness, and continuous monitoring during operation to ensure safety and longevity.

### 5.5.3 Mechanical responses

The mechanical responses of jacket foundations across varying water depths are analyzed in this section, with a focus on the distribution characteristics of

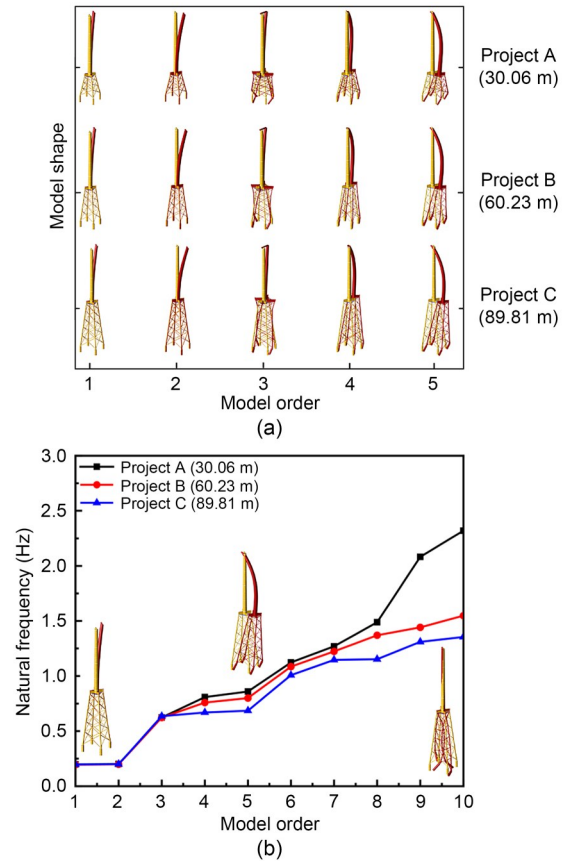


**Fig. 15** (a) Model shapes of jacket foundations under varying water depths at the first five models; (b) natural frequencies of jacket foundations under varying water depths at the first 10 models

jacket member UC value, fatigue damage, and the axial compression and uplift loads on the pile foundations. Fig. 16 presents the jacket member UC values and fatigue damage of the jacket foundations at varying water depths. The overall distribution patterns are quite similar at different water depths. Under extreme load conditions, the maximum jacket member UC values are concentrated at the bottom layer of the jacket, indicating that this region experiences the highest and most critical stress; thus, special attention should be given to the strength and stability of the bottom-layer members of the jacket. As shown in Fig. 16b, the maximum fatigue damage is mainly concentrated in the upper part of the jacket, and the location of maximum fatigue damage tends to shift upward with increasing water depth. For example, at a water depth of 30.06 m (Project A), the maximum fatigue damage occurs at the third-level node (counting from top to bottom), whereas at 60.23 m (Project B) and 89.81 m (Project C), it occurs at the second-level node.

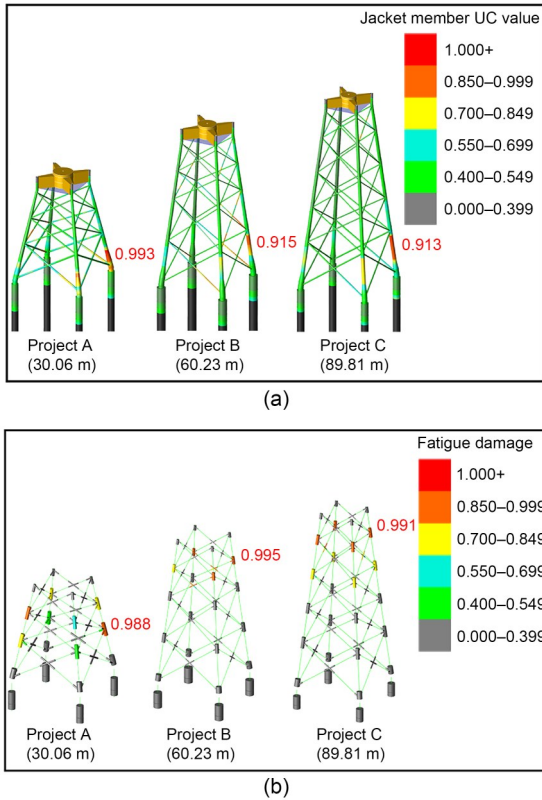


**Fig. 16 (a) Jacket member UC value and (b) fatigue damage of jacket foundations under varying water depths. Reference to color refers to the online version of this figure**

Fig. 17 showcases the axial compression and uplift loads on the pile at varying water depths. As the water depth increases, both the axial compression and uplift loads significantly increase. The increase in compression load is mainly due to the added self-weight of the upper jacket structure. When the water depth rises from 30.06 to 89.81 m, the compression load increases from 27834.4 to 45036.6 kN, representing an increase of 61.80%; this is significantly smaller than the percentage increase in water depth (which was from 30.06 to 89.81 m—a 198.77% increase). Regarding the uplift load, as the water depth increases from 30.06 to 89.81 m, the uplift load increases from 17197.3 to 31563.2 kN, representing an 83.54% rise—this was higher than the rate of increase of the compression load. The uplift load on the pile foundation is mainly caused by horizontal environmental loads such as wind, waves, and currents. Additionally, the load ratio of uplift to compression increases with water depth, rising from 0.62 at 30.06 m to 0.70 at 89.81 m. Such data indicate that horizontal environmental loads have a greater influence on the jacket foundation as water depth increases.

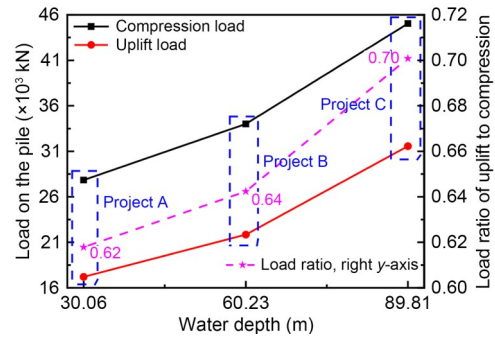


**Fig. 17 Compression load and uplift load on the pile, as well as the load ratio of uplift to compression under varying water depths**

## 6 Conclusions

Based on three real engineering projects at varying water depths, we integrated a SACS-based parametric modeling and analysis framework with a GA optimization strategy to establish an experience-guided optimization model for jacket foundations of OWTs. To address this optimization problem, which has high dimensionality and stringent constraints, a tailored population initialization strategy was proposed. The optimization model’s performance was systematically evaluated to validate its applicability and effectiveness in jacket foundation design. Furthermore, a comparative analysis among the optimized designs corresponding to three different water depths was conducted to investigate the influence of water depth on the jacket foundation, offering valuable insights for the design of jacket foundations in deep-sea environments. The main conclusions can be drawn as follows:

(1) By integrating engineering experience-based solutions into the initial population, the hybrid initialization strategy enabled efficient and feasible starting points for the optimization. The proposed optimization model effectively reduced the required jacket foundation mass across varying water depths by 18.66%, 20.98%, and 17.22% for 30.06, 60.23, and 89.81 m, respectively. Over 60% of the total mass reduction occurred within the first 20 generations, indicating rapid convergence.

(2) A comprehensive analysis of the design constraints revealed that the fatigue life and first natural frequency are the dominant limiting factors across all water depths. The GA framework ensured structural safety and code compliance, with the fatigue life consistently

approaching its lower limit, and the frequency constraints becoming more critical in deeper waters. Uplift bearing capacity also emerged as a key constraint.

(3) The optimization process showed rapid convergence for the jacket's top and bottom spacings, while the structural and pile-related parameters converged more gradually. The key design variables exhibited clear depth-dependent evolution during the optimization. With increasing water depth, larger bottom spacings, thicker main legs, and longer piles were required to ensure structural stability and uplift resistance.

(4) Water depth was found to have a significant impact on the required jacket foundation mass, which increased by 122.94% from 30.06 to 89.81 m of depth. Also, jacket foundations demonstrated a clear competitive advantage in shallow to moderate water depths. The current most cost-effective floating foundation exhibits unit weights per MW that are 97.51% and 35.74% higher than those of jacket foundations at water depths of 60.23 and 89.81 m, respectively. The applicable water-depth threshold between jacket and floating foundations is estimated to be about 100 m.

(5) As water depth increased, the taller jacket foundation—which is characterized by reduced structural stiffness—faced more intense wind, wave, and current forces, resulting in larger structural vibrations. Deeper waters lead to higher stresses in bottom members, an upward shift in the location of maximum fatigue damage, and significantly higher axial pile loads, particularly uplift forces. These trends highlight the escalating impact of horizontal environmental loads with water depth, emphasizing the need for enhanced structural design focused on bottom strength and upper fatigue resistance.

The proposed optimization model for jacket foundations of OWTs effectively integrates engineering design experience with numerical analysis through heuristic algorithms. It reveals designs with substantially reduced jacket foundation mass that still ensure structural performance, offering substantial economic benefits for offshore wind engineering projects.

### Acknowledgments

This study is supported by the Key R&D Program of Zhejiang Province of China (No. 2025C01172).

### Author contributions

Jiajia HUANG, Lizhong WANG, and Lilin WANG designed the research. Tao JIN, Jianwu HUANG, Shasha SONG,

and Chaoqun ZUO processed the corresponding data. Jiajia HUANG wrote the first draft of the manuscript. Wei DAI and Zhen GUO helped to organize the manuscript. Lizhong WANG, Lilin WANG, and Zhen GUO revised and edited the final version.

### Conflict of interest

Lizhong WANG is an Editorial Board member of this journal, and is NOT involved in the editorial review or the decision to publish this article. Jiajia HUANG, Tao JIN, Jianwu HUANG, Shasha SONG, Wei DAI, Chaoqun ZUO, Lizhong WANG, Lilin WANG, and Zhen GUO declare that they have no conflict of interest.

### References

- Achmus M, Kuo YS, Abdel-Rahman K, 2009. Behavior of monopile foundations under cyclic lateral load. *Computers and Geotechnics*, 36(5):725-735.  
<https://doi.org/10.1016/j.compgeo.2008.12.003>
- AlHamaydeh M, Barakat S, Nasif O, 2017. Optimization of support structures for offshore wind turbines using genetic algorithm with domain-trimming. *Mathematical Problems in Engineering*, 2017(1):5978375.  
<https://doi.org/10.1155/2017/5978375>
- American Petroleum Institute (API), 2019a. Planning, Designing, and Constructing Fixed Offshore Platforms—Working Stress Design. API Publishing, Washington, USA.
- American Petroleum Institute (API), 2019b. Planning, Designing, and Constructing Fixed Offshore Platforms—Load and Resistance Factor Design. API Publishing, Washington, USA.
- Benítez-Suárez B, Quevedo-Reina R, Álamo GM, et al., 2025. PSO-based design and optimization of jacket substructures for offshore wind turbines. *Marine Structures*, 101:103759.  
<https://doi.org/10.1016/j.marstruc.2024.103759>
- Cheng XL, Li Y, Mu K, et al., 2024. Seismic response of tripod suction bucket foundation for offshore wind turbine in sands. *Soil Dynamics and Earthquake Engineering*, 177:108353.  
<https://doi.org/10.1016/j.soildyn.2023.108353>
- Chew KH, Tai K, Ng EYK, et al., 2016. Analytical gradient-based optimization of offshore wind turbine substructures under fatigue and extreme loads. *Marine Structures*, 47: 23-41.  
<https://doi.org/10.1016/j.marstruc.2016.03.002>
- Det Norske Veritas (DNV), 2021. Support Structures for Wind Turbines, DNV-ST-0126. DNV, Oslo, Norway.
- Du YM, Kong DQ, Wang SL, et al., 2023. Fatigue analysis of jacket foundations for offshore wind turbines. *Rock and Soil Mechanics*, 44(12):3639-3652 (in Chinese).  
<https://doi.org/10.16285/j.rsm.2022.1709>
- Duan BS, Guo CQ, Liu H, 2022. A hybrid genetic-particle swarm optimization algorithm for multi-constraint optimization problems. *Soft Computing*, 26(21):11695-11711.  
<https://doi.org/10.1007/s00500-022-07489-8>
- Esteban MD, Couñago B, López-Gutiérrez JS, et al., 2015. Gravity based support structures for offshore wind turbine generators: review of the installation process. *Ocean Engineering*, 110:281-291.  
<https://doi.org/10.1016/j.oceaneng.2015.10.033>
- Esteban MD, López-Gutiérrez JS, Negro V, 2019. Gravity-based

- foundations in the offshore wind sector. *Journal of Marine Science and Engineering*, 7(3):64.  
<https://doi.org/10.3390/jmse7030064>
- Feng S, Song YP, Zhang RX, 2000. Optimum design of structure shape for offshore jacket platforms. *China Ocean Engineering*, 14(4):435-445.  
<https://doi.org/10.3321/j.issn:0890-5487.2000.04.004>
- Gavin K, Igoe D, Doherty P, 2011. Piles for offshore wind turbines: a state-of-the-art review. *Proceedings of the Institution of Civil Engineers-Geotechnical Engineering*, 164(4):245-256.  
<https://doi.org/10.1680/geng.2011.164.4.245>
- Gentils T, Wang L, Kolios A, 2017. Integrated structural optimisation of offshore wind turbine support structures based on finite element analysis and genetic algorithm. *Applied Energy*, 199:187-204.  
<https://doi.org/10.1016/j.apenergy.2017.05.009>
- Goldberg DE, 1989. Genetic Algorithms in Search, Optimization and Machine Learning. Addison-Wesley Longman Publishing, Boston, USA.
- Greco S, Ibsen LB, Barari A, 2021. Winkler springs for axial response of suction bucket foundations in cohesionless soil. *Soils and Foundations*, 61(1):64-79.  
<https://doi.org/10.1016/j.sandf.2020.10.010>
- Hong S, McMorland J, Zhang HX, et al., 2024. Floating offshore wind farm installation, challenges and opportunities: a comprehensive survey. *Ocean Engineering*, 304:117793.  
<https://doi.org/10.1016/j.oceaneng.2024.117793>
- Jalbi S, Bhattacharya S, 2020. Concept design of jacket foundations for offshore wind turbines in 10 steps. *Soil Dynamics and Earthquake Engineering*, 139:106357.  
<https://doi.org/10.1016/j.soildyn.2020.106357>
- Jindal S, Rahmanli U, Aleem M, et al., 2024. Geotechnical challenges in monopile foundations and performance assessment of current design methodologies. *Ocean Engineering*, 310:118469.  
<https://doi.org/10.1016/j.oceaneng.2024.118469>
- Li D, Sun T, Yi C, et al., 2025. Development of deep-sea floating wind power technology. *Strategic Study of CAE*, 27(2):108-122 (in Chinese).  
<https://doi.org/10.15302/J-SSCAE-2024.12.024>
- Li ZC, Hu P, Ma JX, et al., 2022. Analysis and prospect of offshore wind power development in China. *China Offshore Oil and Gas*, 34(5):229-236 (in Chinese).  
<https://doi.org/10.11935/j.issn.1673-1506.2022.05.026>
- Li ZY, Xu B, Yuan GK, 2024. Optimization for offshore prestressed concrete-steel hybrid wind turbine support structure with pile foundation using a parallel modified particle swarm algorithm. *Journal of Marine Science and Engineering*, 12(5):826.  
<https://doi.org/10.3390/jmse12050826>
- Liu YC, Li SW, Yi Q, et al., 2016. Developments in semi-submersible floating foundations supporting wind turbines: a comprehensive review. *Renewable and Sustainable Energy Reviews*, 60:433-449.  
<https://doi.org/10.1016/j.rser.2016.01.109>
- Luh GC, Lin CY, 2008. Optimal design of truss structures using ant algorithm. *Structural and Multidisciplinary Optimization*, 36(4):365-379.  
<https://doi.org/10.1007/s00158-007-0175-6>
- Oh KY, Nam W, Ryu MS, et al., 2018. A review of foundations of offshore wind energy converters: current status and future perspectives. *Renewable and Sustainable Energy Reviews*, 88:16-36.  
<https://doi.org/10.1016/j.rser.2018.02.005>
- Piirainen A, de Andres A, Hamilton S, 2020. E&P Offshore: Fixed or Floating Foundations—Which Brings Value for Money in Deeper Water?  
<https://www.hartenergy.com/exclusives/ep-offshore-fixed-or-floating-foundations-which-brings-value-money-deeper-water-188314>.
- Rizk-Allah RM, Snášel V, Deng XF, et al., 2024. Topological optimization of offshore wind farm cable routing system based on an improved equilibrium optimization algorithm. *Ocean Engineering*, 313:119539.  
<https://doi.org/10.1016/j.oceaneng.2024.119539>
- Saka MP, Hasançebi O, Eser H, et al., 2025. Historical evolution of structural optimization techniques for steel skeletal structures including industrial design applications. *Engineering Optimization*, 57(1):69-129.  
<https://doi.org/10.1080/0305215X.2024.2390130>
- Shemshaki E, Haddad MH, Mashayekhi M, et al., 2025. A novel hybrid metaheuristic MPA-PSO to optimize the properties of viscous dampers. *Buildings*, 15(8):1330.  
<https://doi.org/10.3390/buildings15081330>
- Shi W, Park H, Chung C, et al., 2013. Load analysis and comparison of different jacket foundations. *Renewable Energy*, 54:201-210.  
<https://doi.org/10.1016/j.renene.2012.08.008>
- Syalsabila F, Prastianto RW, Rosyid DM, 2022. Sizing optimization using genetic algorithm to achieve minimal offshore structure. *Rekayasa*, 15(2):129-136.  
<https://doi.org/10.21107/rekayasa.v15i2.15102>
- Tian XJ, Sun XY, Liu GJ, et al., 2022. Optimization design of the jacket support structure for offshore wind turbine using topology optimization method. *Ocean Engineering*, 243:110084.  
<https://doi.org/10.1016/j.oceaneng.2021.110084>
- Wang L, Liu YG, Li ZS, et al., 2023. Non-probabilistic reliability-based topology optimization (NRBTO) scheme for continuum structures based on the strength constraint parameterized level set method and interval mathematics. *Thin-Walled Structures*, 188:110856.  
<https://doi.org/10.1016/j.tws.2023.110856>
- Williams R, Zhao F, 2024. Global Offshore Wind Report 2024. Global Wind Energy Council, Brussels, Belgium.
- Yu Y, Wei MX, Yu JX, et al., 2023. Reliability-based design method for marine structures combining topology, shape, and size optimization. *Ocean Engineering*, 286:115490.  
<https://doi.org/10.1016/j.oceaneng.2023.115490>
- Zhou YM, Zhang JH, Long K, et al., 2025. Topology optimization on a jacket structure for offshore wind turbines by altering structural design domain. *Applied Ocean Research*, 154:104421.  
<https://doi.org/10.1016/j.apor.2025.104421>

## Electronic supplementary materials

Sections S1–S3, Tables S1–S7, Figs. S1–S6, Eqs. (S1)–(S10)